Molecular Vision 2006; 12:1516-25 <http://www.molvis.org/molvis/v12/a174/>
Received 22 March 2006 | Accepted 8 November 2006 | Published 5 December 2006

Arrestin residues involved in the functional binding of arrestin to phosphorylated, photolyzed rhodopsin

Maria T. Ascano,[1] W. Clay Smith,[3] Susan K. Gregurick,[2] Phyllis R. Robinson[1]

(Dr. Smith and Dr. Robinson contributed equally to this publication)

[1]Department of Biological Sciences, [2]Department of Chemistry and Biochemistry, University of Maryland, Baltimore County, Baltimore, MD, [3] Department of Ophthalmology, Department of Neuroscience, University of Florida, Gainesville, FL

Purpose: The purpose of our study was to determine whether arrestin residues previously predicted by computational modeling to interact with an aspartic acid substituted rhodopsin tail are actually involved in interactions with phospho-residues on the rhodopsin cytoplasmic tail.
Methods: We generated arrestin mutants with altered charges at predicted positions. These mutants were then tested for the ability to inhibit rhodopsin using both direct binding assays, as well as functional assays involving transducin inhibition assays.
Results: Our results demonstrate that the computer-predicted residues are indeed involved in both the ability of the low-affinity state of arrestin to bind to rhodopsin as well as the ability of arrestin to be induced into a higher-affinity state in a phospho-residue-dependent manner.
Conclusions: Our results also suggest that positions K14, K15, R29, H301, and K300 on arrestin interact with the phosphorylated carboxyl tail of rhodopsin and that this translates to the efficient activation of arrestin.

The rhodopsin-activated phototransduction cascade is one of the most studied G protein-coupled receptor (GPCR) systems [1-5]. Once rhodopsin absorbs a photon of light, it undergoes conformational changes that eventually lead to the formation of an active conformation, termed metarhodopsin II (Meta II). In this conformation, rhodopsin is able to activate its coupled G protein, transducin. As with other GPCR receptors, upon formation of its active conformation, rhodopsin is immediately targeted for deactivation through a stereotypical two-step process: phosphorylation by a G protein-coupled receptor kinase (GRK) followed by binding of a representative member of the arrestin-family of proteins. In the case of vertebrate rhodopsin, the Meta II conformation is recognized and phosphorylated by a specific serine/threonine protein kinase, rhodopsin kinase (RK) [6,7]. Phosphorylation partially inactivates rhodopsin, making it less efficient at activating transducin. Nevertheless, complete and rapid deactivation of the active receptor requires the binding of a second regulatory protein called arrestin, the first member of the arrestin family of proteins to be identified [8].

Arrestin deactivates rhodopsin by directly competing with transducin for the rhodopsin cytoplasmic loops. Binding of arrestin to light-activated rhodopsin is dependent on the phosphorylation of rhodopsin by RK [8,9]. There are three mechanistic models that describe the interaction of arrestin and phospho-rhodopsin. The first model articulated by Gurevich and co-workers posits that in the dark, arrestin exists in an inactive, low-affinity binding state. The interaction between arrestin and the phosphorylated residues on the rhodopsin tail induces a large conformational change in arrestin involving the N-and C-terminal domains, which increases the affinity of arrestin for photo-activated rhodopsin, presumably by exposing buried regions within arrestin that are able to stabilize its interaction with the rhodopsin cytoplasmic loops [10,11]. Shilton et al. [12] suggest that this conformational change is small and involves arrestin's loops. Finally, Liang et al. [13] suggests that the N-and C-terminal cavities bind to rhodopsin dimers. This paper assumes that the interaction between arrestin and the phosphorylated residues on the rhodopsin tail induces a conformational change in arrestin that can then bind phosphorlyated metarhodopsin II [14].

There are several compelling lines of evidence that suggest at least three phospho-residues are required for proper deactivation [15-17]. Although several studies suggest that it is the overall number of phosphates that affects arrestin binding and therefore rhodopsin deactivation, in vitro data from our laboratories, as well as studies by others, have shown that the position of the phospho-residues, or any negative charge on the rhodopsin tail, can greatly affect the ability of arrestin to inhibit transducin activation by photolyzed phosphorylated rhodopsin [16,18]. The question remains as to how the position of the phospho-residues on the rhodopsin cytoplasmic tail affects arrestin's ability to inhibit rhodopsin activity. This investigation aims to answer this question by characterizing residues on arrestin that were found to interact with negatively charged residues on the rhodopsin tail during computational simulations.

Correspondence to: Phyllis Robinson, Department of Biological Sciences, University of Maryland, Baltimore County, 1000 Hilltop Circle, Baltimore, MD 21250; Phone: (410) 455-2977; FAX: (410) 455-3875; email: probinso@umbc.edu

We previously developed a computational strategy that allowed us to make predictions of potential sites of interaction between the arrestin and the rhodopsin cytoplasmic tail [13]. We simulated the interaction between arrestin 1CF1 [19] and a negatively charged rhodopsin tail using an all-atom Monte-Carlo Simulated Annealing (MC-SA) approach [20]. This approach determines optimal structure using energy optimization algorithms, allowing us to probe for specific residues that form interactions between arrestin and the rhodopsin cytoplasmic tail. Optimally, we would have used this approach to predict possible interactions between arrestin and the phospho-residues on rhodopsin's carboxyl tail. However, because calculations for phosphate force fields do not currently exist, we performed the simulations with rhodopsin peptides with all seven phosphorylatable sites substituted with either aspartic or glutamic acid residues. We have previously shown that aspartic and glutamic acid residues on the rhodopsin tail can increase the affinity of arrestin for unphosphorylated rhodopsin [21]. This approach allowed us to examine the interaction between the negatively charged rhodopsin tail and arrestin.

The MC-SA simulations predicted that negative charged residues at positions 334 and 340 on the rhodopsin tail interact with Lys^{15}, Arg^{29}, Lys^{300}, and His^{301} positively charged residues on arrestin (see Figure 1) [13]. Prior to our studies, Lys^{15} was shown to be necessary for arrestin's phosphate sensitivity [22]. In this current study, we characterize the role of arrestin residues Arg^{29}, His^{301}, and Lys^{300} during arrestin activation using in vitro biochemical techniques. We generated mutations that either neutralized or reversed the charges at these amino acid positions and tested the ability of these arrestin mutants to bind rhodopsin, inhibit transducin activation, and undergo conformational changes as indicated by susceptibility of the arrestin carboxyl tail to tryptic digestion.

METHODS

Preparation of arrestin mutants: Point mutations were introduced into the cDNA of bovine visual arrestin by mega-priming PCR [23]. An N-terminal His_6-tag was placed immediately after the initiating methionine of arrestin. Mutated arrestin cDNA's were cloned into the shuttle vector pPIC-Za (Invitrogen) for expression in *Pichia pastoris* strain GS115. DNA sequencing on both strands confirmed all the mutations. Expressed proteins were purified by affinity chromatography over nickel-agarose (His-select, Sigma, St Louis, MO), followed by heparin affinity chromatography (heparin-sepharose, Amersham, Piscataway, NJ) as previously described [24].

Preparation of p44 mutants: N-terminal His-tagged bovine p44 cDNA was cloned into pPIC-Zb (Invitrogen, Carlsbad, CA). Site-directed mutagenesis was performed using QuikChange Mutatgenesis protocol (Stratagene) with Pfu Ultra polymerase (Stratagene, La Jolla, CA). Constructs were confirmed and expressed as with arrestin mutants. GS115 clones with p44 gene insertions were confirmed with a PCR screen using 5' and 3' AOX1 primers. Positive clones were grown according to the manufacturer's instruction for expres-

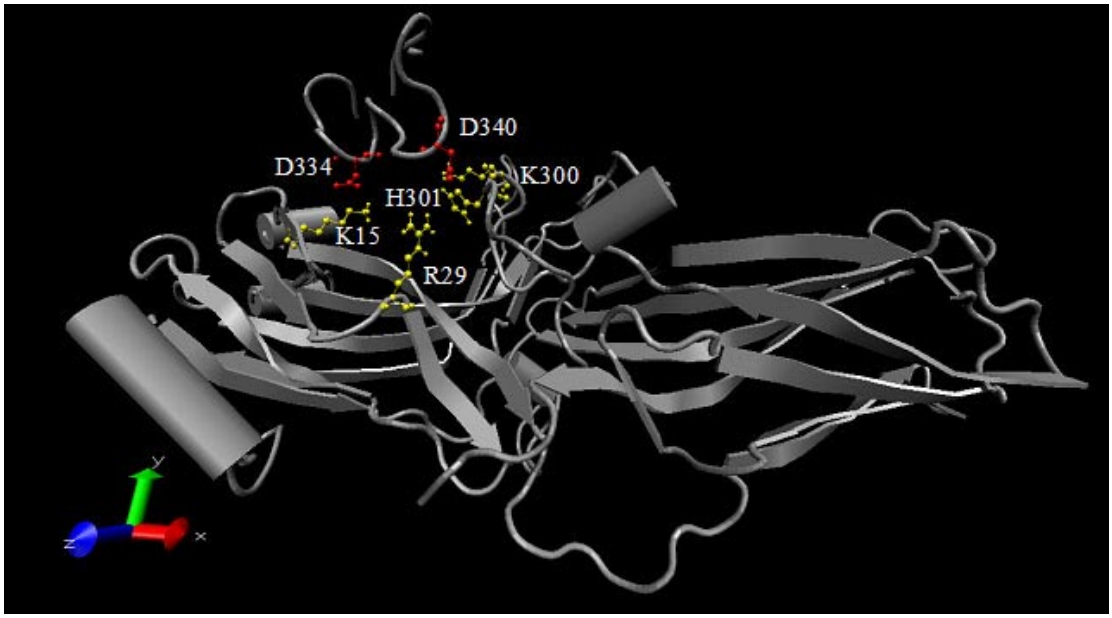

Figure 1. Interactions between arrestin and rhodopsin's cytoplasmic tail. This figure is a representation of the computational simulations of the interactions between arrestin and the rhodopsin cytoplasmic tail. It is a Visual Molecular Dynamics representation [43] of the Monte-Carlo Simulated Annealing simulations previously described in Ling et al. [13]. The interaction between a 20 amino acid rhodopsin C-terminal peptide analog and the arrestin molecule was computationally simulated. The phosphorylatable sites on the peptide were replaced with Asp residues to mimic phospho-residues. This figure depicts the final conformation of both the peptide and arrestin once the simulations were complete. The residues on the rhodopsin peptide designated in red are residues Asp^{334} and Asp^{340} that were found to have a positive interaction with the residues on arrestin, designated in yellow. The yellow residues on arrestin are residues Lys^{15}, Arg^{29}, His^{301}, and Lys^{300}.

sion of proteins in *Pichia pastoris* (Invitrogen). Cells were lysed using a French press (20,000 psi) in 10 mM $NaPO_4$ (pH 6.4) with 300 mM NaCl and 10 mM imidazole. The lysate was centrifuged at 30,000x g for 30 min. The supernatant was loaded onto 10 ml column volume of NTA resin (Qiagen, Valencia, CA) and washed with 20 mM imidazole. p44 was eluted from the NTA column using 250 mM imidazole and loaded onto a 1 ml Hi-Trap™ Heparin column (Amersham). p44 was eluted from the Hi-Trap™ column using 400 mM NaCl in 10 mM HEPES (pH 7.5).

Measurement of Arrestin or p44-mediated deactivation of rhodopsin: The ability of arrestin to functionally bind and inhibit rhodopsin was determined by measuring transducin activation. ^{35}S-γ-GTP filter-binding assays were performed, and arrestin or p44-mediated deactivation was determined as previously described [13]. In arrestin assays, the final arrestin concentration in all reactions was 5 μM. In the p44 assays, the final concentration of p44 in reactions with unphosphorylated rhodopsin was 5 μM and 2 μM in reaction with phosphorylated rhodopsin. The final concentration of transducin for all ^{35}S-γ-GTP assays was between 2.5 and 3.0 μM.

Purification of transducin from bovine rod outer segments: Bovine retinas were obtained from Preston Van Hooser (University of Washington, Seattle, WA) and Shenk Inc. (Seattle, WA). Transducin was purified as previously described [25]. Purified transducin was stored at -20 °C in 50% glycerol in 10 mM Tris-HCl (pH 7.4), 2 mM $MgCl_2$, and 1 mM DTT.

Expression and purification of rhodopsin kinase: Recombinant rhodopsin kinase was expressed and purified as previously described [13].

Tryptic digestion of arrestin: Native arrestin and arrestin mutants were prepared at 4 μM in 50 mM Tris buffer, pH 8.0. TPCK-treated trypsin (Sigma) was added to a final concentration of 20 nM, and the reaction incubated at room temperature. Fully phosphorylated peptide of the C-terminus of bovine rhodopsin (the peptide DDEASTTVSKTETSQVAPA where all S and T residues have been phosphorylated; 7PP) [26] was added to the reaction at indicated concentrations. Aliquots of the reaction were removed and quenched by vortexing with Laemmli sample buffer [27]. Samples were separated using 12% SDS-PAGE, stained with coomassie brilliant blue, and the full-length arrestin quantified by scanning densitometry.

Binding of arrestin and p44 to rhodopsin-containing membranes: Membranes of bovine rod outer segments containing rhodopsin were prepared in unphosphorylated and phosphorylated form as previously described [28]. Arrestin or p44 (3 μM) were mixed with rhodopsin (7 μM) in disc membranes on ice, illuminated on a light box for 2 min, and then centrifuged (40,000x g for 30 min). The pellet was solubilized in Laemmli sample buffer, separated by 12% SDS-PAGE, and stained with coomassie brilliant blue. Arrestin and p44 were quantified by scanning densitometry and normalized to the amount of native arrestin bound to phosphorylated, photolyzed rhodopsin.

RESULTS

Effect of arrestin mutations on deactivation of rhodopsin: We generated arrestin mutants lacking one or more of the predicted contact sites and assayed them using several biochemical assays. Arrestin mutants with single point mutations [Arg^{29}->Glu (R29E-Arr), Lys^{15}->Ala (K15A-Arr), Lys^{300}->Glu or Ala (K300E-Arr or K300A-Arr), and His^{301}->Glu or Ala (H301E-Arr or H301A-Arr)] and multiple point mutations [Lys^{14}->Ala+Lys^{15}->Ala+Arg^{29}->Glu (K14A/K15A/R29E) and

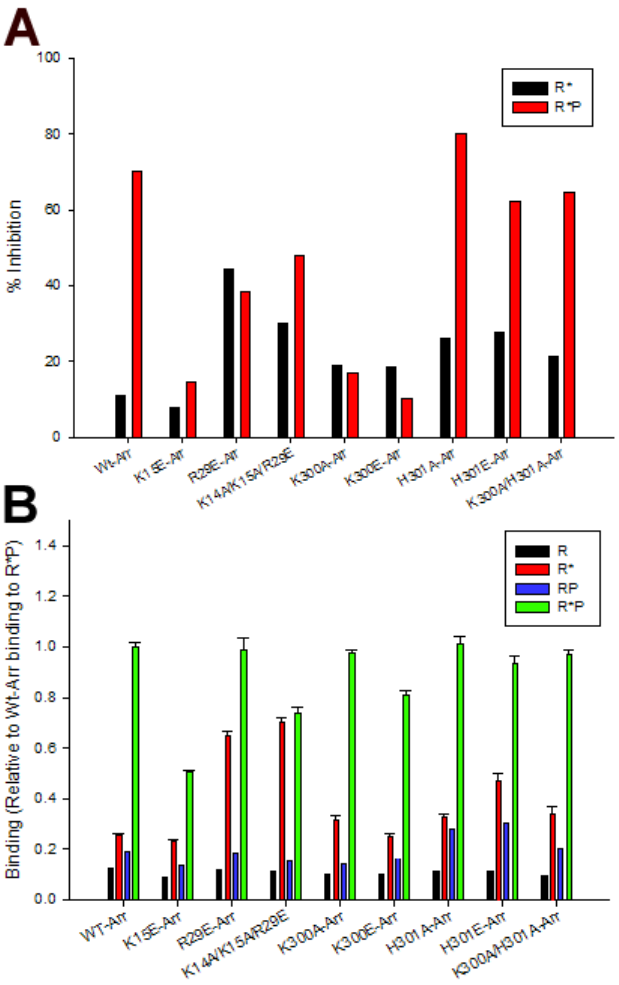

Figure 2. Effect of arrestin mutants on phosphorylated and unphosphorylated rhodopsin. **A**: Arrestin-mediated rhodopsin deactivation. ^{35}S-γ-GTP assays were performed as described in Methods. WT rhodopsin was incubated either with (gray bars) or without (black bars) rhodopsin kinase. Arrestin was then added to a final concentration of 5 μM. Bars are averages from two independent experiments. **B**: Direct binding of arrestin mutants to different phosphorylation and photoactivation states of rhodopsin. The ability of the different arrestin mutants to bind to rhodopsin was determined using co-precipitation studies. Arrestin mutants (4 μM) were incubated with membranes from bovine rod outer segments that contained unphotolyzed unphosphorylated (R), photolyzed unphosphorylated (R*), unphotolyzed phosphorylated (RP) and photolyzed phosphorylated (R*P) rhodopsin (7 μM). Error bars represent SEM (n=4). All binding was normalized to binding of WT-Arr to R*P.

Table 1. Effect of arrestin mutants on photolyzed rhodopsin

	Ability to decrease activity of photolyzed rhodopsin (relative to WT-Arr)		Ability to bind photolyzed rhodopsin (relative to WT-Arr)	
Arrestin mutants	Unphosphorylated rhodopsin	Phosphorylated rhodopsin	Unphosphorylated rhodopsin	Phosphorylated rhodopsin
WT	1.00	1.00	1.00	1.00
K15E	0.52	0.19	0.90	0.50
R29E	2.95	0.52	2.53	0.98
K14A/K15A/R29E	2.00	0.65	2.75	0.73
K300A	1.28	0.22	1.24	0.97
K300E	1.23	0.13	0.98	0.80
H301A	1.75	1.08	1.28	1.01
H301E	1.84	0.84	1.83	0.93
K300A/H301A	1.42	0.88	1.32	0.96

The ability of arrestin mutants to decrease activity of photolyzed rhodopsin was determined by measuring transducin activation as described in the methods and expressed relative to wild type arrestin. The final arrestin concentration in all reactions was 5 μM and the final concentration of transducin was between 2.5 and 3.0 μM. The ability of arrestin mutants to bind to photolyzed rhodospsin was measured by a centrifugation assay as described in the methods and expressed relative to wild type arrestin. The final arrestin concentration was 3 μM and the final concentration of rhodopsin in the reaction was 7 μM.

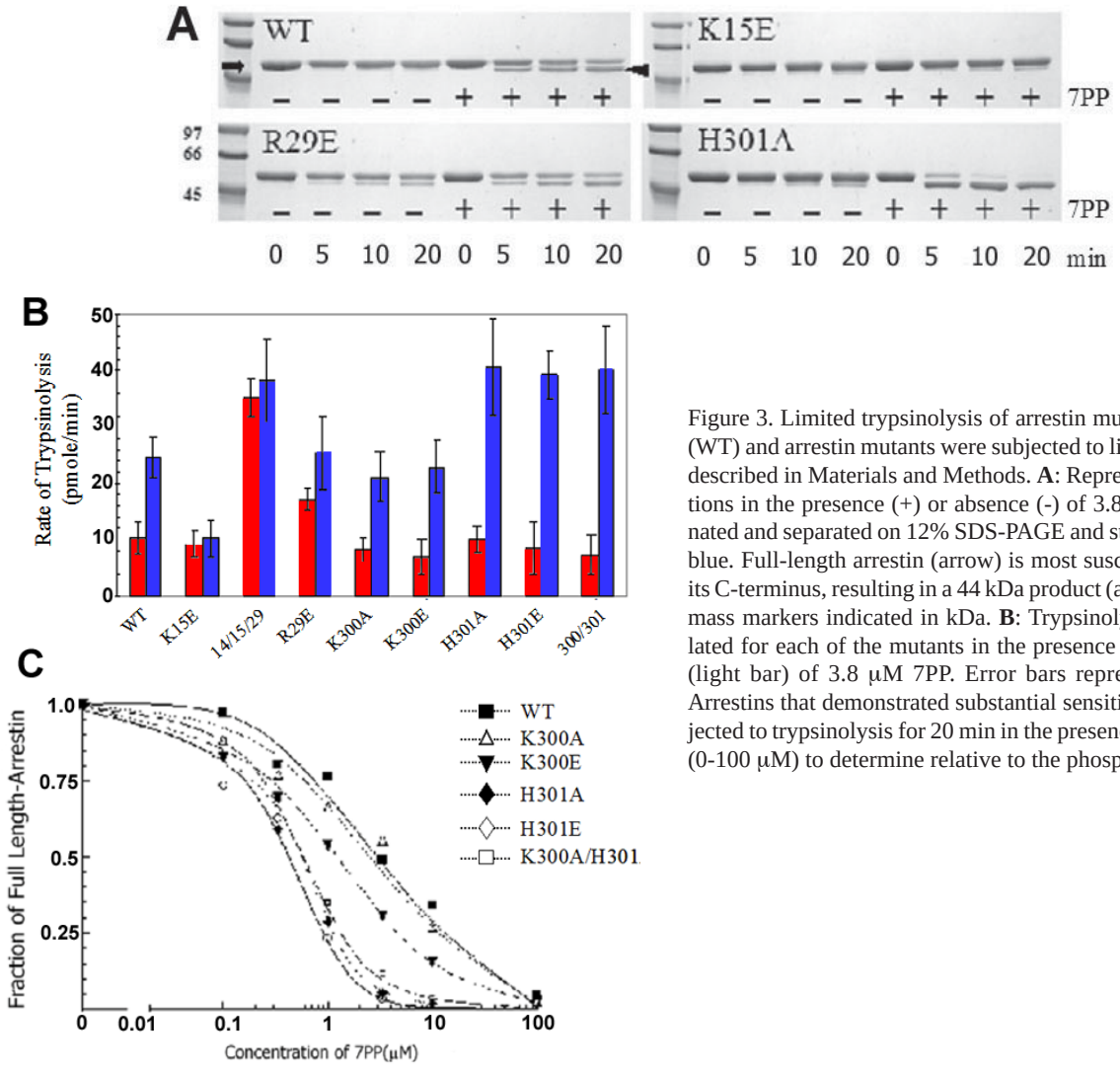

Figure 3. Limited trypsinolysis of arrestin mutants. Native arrestin (WT) and arrestin mutants were subjected to limited trypsinolysis as described in Materials and Methods. **A**: Representative tryptic reactions in the presence (+) or absence (-) of 3.8 μM 7PP were terminated and separated on 12% SDS-PAGE and stained with coomassie blue. Full-length arrestin (arrow) is most susceptible to cleavage at its C-terminus, resulting in a 44 kDa product (arrowhead); molecular mass markers indicated in kDa. **B**: Trypsinolysis rates were calculated for each of the mutants in the presence (dark bar) or absence (light bar) of 3.8 μM 7PP. Error bars represent SEM (n=3). **C**: Arrestins that demonstrated substantial sensitivity to 7PP were subjected to trypsinolysis for 20 min in the presence of a titration of 7PP (0-100 μM) to determine relative to the phospho-peptide.

Lys[300]->Ala+His[301]->Ala (K300A/H301A-Arr)] were generated with an N-terminal His_6-tag, expressed in *Pichia*, and purified to >95% homogeneity. Their interaction with rhodopsin was tested indirectly using an assay to measure the inhibition of transducin activation (Figure 2A and Table 1). K300A-Arr, K300E-Arr, and K15E-Arr show decreased arrestin-mediated inhibition of phosphorylated rhodopsin as compared to WT-Arr. This is wild type bovine arrestin with a His[6] tag on the N-terminal end, expressed and purified as described in the methods section. As shown previously in other studies [22], the loss of Lys[15] compromises the ability of this arrestin mutant to bind to phosphorylated rhodopsin. In our assay K15E-Arr exhibits about 80% decrease in ability to deactivate phosphorylated rhodopsin compared to WT-Arr. Likewise, K300A-Arr and K300E-Arr also show an 80% decrease in ability to deactivate phosphorylated rhodopsin compared to WT arrestin. The importance of position K300 was also recently reported [29]. Nevertheless, the arrestin mutants K15E-Arr, K300A-Arr, and K300E-Arr still deactivate unphosphorylated rhodopsin to the same extent as WT-Arr. Mutation of His[301] to an alanine residue (H301A-Arr) does not change arrestin's ability to deactivate phosphorylated rhodopsin compared to WT-Arr, while mutation of His[301] to a glutamic acid residue decreases arrestin's ability to inhibit phospho-rhodopsin to 85% of inhibition by WT-Arr. However, both His[301] mutants show higher inhibition of unphosphorylated rhodopsin than WT-Arr. Inhibition of unphosphorylated rhodopsin by both H301A-Arr and H301E-Arr is almost twice as high as the level of WT arrestin deactivation. Mutation of His[301] to an alanine can rescue the K300A-Arr phenotype. The double mutant K300A/H301A-Arr shows levels of deactivation of phosphorylated rhodopsin similar to that of the H301E-Arr mutant. Both Arg[29] mutants, R29E-Arr and K14A/K15A/R29E, inhibit

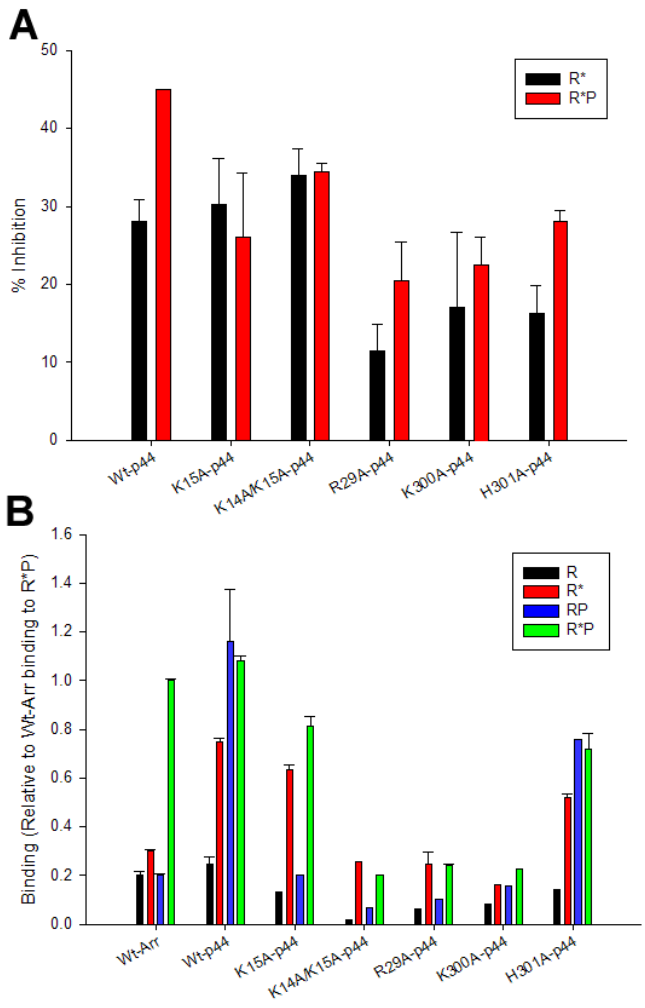

Figure 4. The inhibitory effect of p44 mutants on phosphorylated and unphosphorylated WT rhodopsin. **A**: p44-mediated rhodopsin deactivation. Assays were performed as described in Figure 2 legend. p44 was added to a final concentration of 2 μM (phosphorylated rhodopsin) and 5 μM (unphosphorylated rhodopsin). Error bars represent SD (n=3-4). **B**: Direct binding of p44 mutants to different phosphorylation and photoactivation states of rhodopsin. Assays were performed as described in Figure 2 legend. All binding was normalized to binding of WT-Arr to R*P.

Table 2. Effect of p44 mutants on photolyzed rhodopsin

	Ability to decrease activity of photolyzed rhodopsin (relative to WT p44)		Ability to bind photolyzed rhodopsin (relative to WT p44)	
p44 Mutants	Unphosphorylated rhodopsin	Phosphorylated rhodopsin	Unphosphorylated rhodopsin	Phosphorylated rhodopsin
WT p44	1.00	1.00	1.00	1.00
K15A	1.08	0.60	0.84	0.75
K14A/K15A	1.21	0.79	0.34	0.18
R29A	0.41	0.47	0.33	0.22
K300A	0.60	0.51	0.21	0.20
H301A	0.58	0.64	0.69	0.66

The ability of p44 mutants to decrease activity of photolyzed rhodopsin was determined by measuring transducin activation as described in the methods and expressed relative to wild type p44. The final concentration of p44 in reactions with unphosphorylated rhodopsin was 5 μM and 2 μM in reaction with phosphorylated rhodopsin and the final concentration of transducin was between 2.5 and 3.0 μM. The ability of p44 mutants to bind to photolyzed rhodospsin was measured by a centrifugation assay as described in the methods and expressed relative to wild type arrestin. The final p44 concentration was 3 μM and the final concentration of rhodopsin in the reaction was 7 μM.

unphosphorylated rhodopsin to a greater extent than WT-Arr. This is reflective of other arrestin mutations that either destabilize the arrestin carboxyl tail from the main arrestin body or mutations that destabilize the charge equilibrium within the arrestin polar core [22,30,31]. However, unlike other arrestin mutants, the Arg^{29} mutations not only increase arrestin binding to unphosphorylated rhodopsin but also decrease binding to phosphorylated rhodopsin relative to WT-Arr. The mutations that increase arrestin inhibition of unphosphorylated rhodopsin allude to the possibility that those residues function to maintain arrestin in an inactive conformation, while those that result in decreased inhibition of phosphorylated rhodopsin suggest the role of those residues in arrestin's activation.

Measurement of direct binding of arrestin mutants to rhodopsin: To analyze the direct binding of arrestin mutants to rhodopsin we performed co-precipitation studies. As seen in Figure 2B (and Table 1), WT-Arr shows little binding to unphotolyzed rhodopsin, whether phosphorylated (RP) or unphosphorylated (R). It does, however, bind to photolyzed rhodopsin as long as it is phosphorylated (R*P). Like WT-Arr, none of the arrestin mutants bind at high levels to R or RP. Experiments in other laboratories have demonstrated that the neutralization of the Lys^{15} charge leads to decreased binding of arrestin to phosphorylated rhodopsin [22]. Consistent with those studies, the loss of Lys^{15} (K15A-Arr) in our experiments leads to the decrease in binding of arrestin to R*P. Binding of the triple arrestin mutant K14A/K15A/R29E to R*P, however, is significantly higher than that of K15E to R*P. Like the triple mutant, R29E-Arr binds to catalytically active photolyzed rhodopsin (R*) to a greater extent than WT-Arr. Both R29E-Arr and K14A/K15A/R29E show almost three times more binding to R* (as know as MetaII) than WT-Arr. Likewise, there is an increase in binding of H301E-Arr to R* as compared to WT-Arr.

Mutation of Lys^{300} does not seem to greatly affect the ability of arrestin to bind to R*P. The binding of K300A to R*P is indistinguishable from WT, whereas the binding of K300E-Arr to R*P is 80% of the WT level. This is consistent with a recent study that reports binding of the K300E-Arr mutant to 70% of wild type values [29].

Tryptic digestion of arrestin mutants: To directly test the responsiveness of the arrestin mutants to the phospho-residues on the rhodopsin cytoplasmic tail, we performed tryptic digest studies [21] (Figure 3). WT-Arr is relatively insensitive to trypsin digestion in the absence of 7PP, but is rapidly digested after brief incubation periods with 3.8 μM 7PP. K15E-Arr shows decreased sensitivity to 7PP such that even with extended incubation periods with 3.8 μM 7PP there is little susceptibility of its carboxyl tail to trypsin. Trypsinolysis analysis of K300A-Arr and K300E-Arr shows that the rate of trypsin digestion of the carboxyl tail of these two arrestin mutants follows a similar profile as WT-Arr both in the presence and absence of 7PP (Figure 3B). The carboxyl tails of arrestin mutants H301A-Arr, H301E-Arr and K300A/H301A-Arr are digested at a similar rate as WT-Arr in the absence of the 7PP (Figure 3B). However, the rate of digestion of all three mutants is much faster than WT-Arr in the presence of the 7PP. We titrated the concentration of 7PP in the tryptic digest reactions to quantify the relative stability of the carboxyl tail between the His^{301} mutants. The results show that H301A, H301E and K300A/H301A are about 5 to 6 fold more responsive to 7PP than WT-Arr (Figure 3C). Trypsinolysis analysis of the Arg^{29} mutants, R29E-Arr and K14A/K15A/R29E, reveal that both mutants are susceptible to tryptic digest even in the absence of the phospho-peptide.

Effect of mutations on p44-mediated deactivation of rhodopsin: To directly examine the role these arrestin residues play after the displacement of the carboxyl tail, we generated p44 mutants with alanine substitutions of the corresponding residues. We substituted residues Lys^{14}, Lys^{15}, Arg^{29}, Lys^{300}, and His^{301} in p44 for alanine residues and tested the effect these mutations had on the ability of p44 to bind and inhibit rhodopsin activity. We tested the ability of the p44 mutants to inhibit the activity of both unphosphorylated and phosphorylated photolyzed rhodopsin in the ^{35}S-γ-GTP filter-binding assay (Figure 4A and Table 2). K15A-p44 and K14A/K15A-p44 show similar inactivation of unphosphorylated rhodopsin as WT-p44. However, they show no increase in percent inhibition upon phosphorylation of rhodopsin. R29A-p44, K300A-p44, and H301A-p44 all show decreased inhibition of both unphosphorylated and phosphorylated rhodopsin relative to WT-p44. Likewise, K300A-p44 and H301A-p44 show decreased inhibition of R*P as compared to WT-p44.

Measurement of direct binding of p44 mutants to rhodopsin: Figure 4B and Table 2 outlines the direct binding studies performed on the p44 mutants. All the p44 mutants show decreased binding to both R* and R*P as predicted by the transducin activation studies. K15A-p44 shows a 15% decrease in binding to R* and a 24% decrease in binding to R*P relative to WT-p44. The double mutant, K14A/K15A-p44 shows a more drastic phenotype with a decrease in binding to R* and R*P of over 80% compared to WT-p44. Both R29A-p44 and K300A-p44 show a marked decrease in binding to both R* and R*P, with an 80% decrease in binding compared to that of WT-p44. H301A-p44 shows a similar binding profile as K15A-p44 with similar decreases in binding to R* and R*P.

DISCUSSION

Phosphorylation of rhodopsin's C-terminus is an important step for arrestin-mediated rhodopsin deactivation. The phosphates induce a conformational change in arrestin that reveals a rhodopsin high-affinity binding site. Although all seven serine and threonine residues on the rhodopsin tail are substrates for RK, it does not appear to be necessary for all seven residues to be phosphorylated for deactivation [15,32-35]. Although an early study suggested that three phosphorylatable sites are sufficient to generate WT deactivation of mouse rhodopsin in vivo [15], a recent study by Doan et al. [36] now suggests reproducible single photon response kinetics may require up to six phosphorylatable sites. In contrast to these in vivo studies with transgenic mice, we have previously found that both the number and position of the phospho-residues on the bovine rhodopsin carboxy tail greatly affects the ability of arrestin

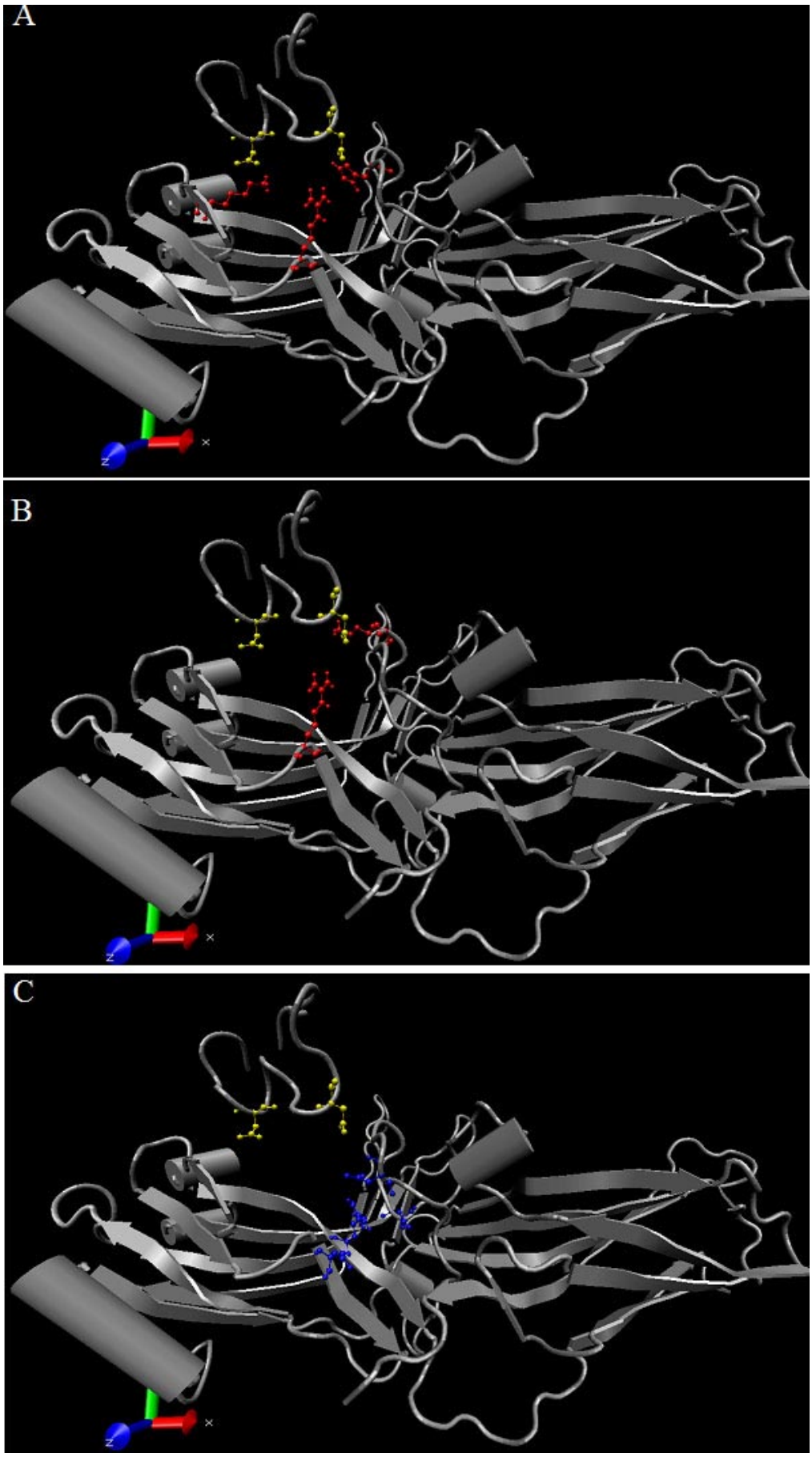

Figure 5. Model for the proposed interactions between arrestin and the phosphorylated rhodopsin cytoplasmic tail. Aspects of this model have been put forth previously by Gurevich and coworkers [44]. Panels are generated using VMD. In this model, arrestin exists alone in a stable low-affinity rhodopsin-binding state due to certain intramolecular interactions that both anchor the arrestin carboxyl tail to the main arrestin body as well as maintain rhodopsin high-affinity binding sites hidden. The role of the phosphorylated residues on the rhodopsin tail is two-fold: (1) displace the arrestin carboxyl tail and (2) generate a conformational change that exposes the high-affinity rhodopsin binding sites. The arrestin carboxyl tail is anchored to the main arrestin body by intramolecular interactions involving His^{301} and Arg^{29} (**A**). Upon displacement of the arrestin carboxyl tail, the negative charges on the rhodopsin tail are initially anchored to arrestin through specific interactions with residues Lys^{15}, Lys^{300}, and Arg^{29} (**B**). However, for efficient rhodopsin inhibition the high-affinity rhodopsin binding sites are required, and these are made available upon disruption of the salt-bridges (**C**) within the polar core, inducing a conformational change in arrestin, revealing the high-affinity binding sites.

to bind and inhibit transducin activation [17]. Our current study therefore attempts to describe the molecular mechanism that underlies the positional requirement of the phospho-residues during the rhodopsin-arrestin interaction.

Previously, we demonstrated that we could use computer simulations to predict specific residue-residue interactions between arrestin and a rhodopsin mutant with all seven phosphorylatable sites replaced with aspartic acid residues [13]. In this study, we expanded our analysis to determine whether the specific arrestin residues that were computationally identified to interact with negative residues on the rhodopsin carboxyl tail are also involved in arrestin's phosphate sensitivity.

Using the current study, in conjunction with the known literature, we suggest a step-wise model for the interaction between negative charges on the rhodopsin tail and arrestin residues. It is already known that the displacement of the arrestin carboxyl tail is a crucial step during arrestin activation [37]. However, high affinity binding of arrestin to rhodopsin requires the disruption of ionic interactions that lie within the arrestin core [31]. Our current study demonstrates that the same residues on arrestin that are targeted for displacement of the carboxyl tail are also required subsequent to the displacement of the tail. These findings explain the positional requirements of phospho-residues found previously [18]. If high-affinity binding of arrestin to rhodopsin requires the simultaneous interaction of phospho-residues with multiple residues on arrestin, then it is possible that both the number and position of the phosphates could affect the arrestin-rhodopsin interaction.

Figure 5 illustrates a model for stepwise activation of arrestin and binding to rhodopsin. Our results suggest that the residues on arrestin that are targeted by the negative residues on the rhodopsin cytoplasmic tail play a role both in anchoring the arrestin carboxyl tail to the main arrestin body as well as stabilizing the arrestin-rhodopsin complex after displacement of the arrestin carboxyl tail.

According to our computational simulations, two residues targeted by the negative charges on the rhodopsin tail are Arg^{29} and His^{301}. Both residues were found to be involved in anchoring the arrestin carboxyl tail to the main arrestin body. Loss of either of these residues leads to an increase in binding of arrestin to unphosphorylated rhodopsin. This increase in binding is also translated to an increase in ability to inhibit transducin activation by unphosphorylated rhodopsin. However, both residues were also found to be involved in the stable binding of p44 and arrestin to phosphorylated rhodopsin, suggesting both residues are still necessary even after displacement of the carboxyl terminal.

Our computational simulations also identified Lys^{14} and Lys^{15} as residues targeted by the negative residues on the rhodopsin cytoplasmic tail. Consistent with other studies, our results show that Lys^{14} and Lys^{15} are necessary for proper displacement of the arrestin carboxyl tail. However, we also find these residues to be necessary for the proper interaction between p44 and phosphorylated rhodopsin suggesting that like Arg^{29} and His^{301}, these two lysine residues are required after displacement of the arrestin tail.

The final residue identified in our computational studies was Lys^{300}. Although we found K300A-Arr and K300E-Arr to have a WT-Arr profile in the tryptic digest studies, we found these mutants to have decreased binding to phosphorylated rhodopsin suggesting that Lys^{300} is required for arrestin's phosphate sensitivity. Its importance for p44's phosphate sensitivity suggests again that this residue is necessary after displacement of the arrestin carboxyl tail. Lys^{300} also lies close to the loop comprised of residues 68-78 when the loop is in the folded down conformation (unit C of the arrestin crystal structure) [38]. This loop has been substantively implicated in the binding of arrestin to photolyzed-phosphorylated rhodopsin [14,39-41]. Perhaps Lys^{300} plays an important role in stabilizing the proper positioning of this mobile loop structure.

The proper alignment of the arrestin residues and the phospho-residues on the rhodopsin tail may function to aid in polar core disruption. Our computational simulations suggested that negative residues at rhodopsin positions 334 and 340 interact with the arrestin residues examined in this current study. However, we know from other studies that the complement of phospho-residues present on the rhodopsin tail is as important as the overall number of phosphorylated rhodopsin residues [42]. Given that arrestin and p44 seem to differentially bind to rhodopsin molecules with different complements of phospho-residues, what may play a bigger role in rhodopsin deactivation in vivo is the sequence in which rhodopsin residues are phosphorylated. With both arrestin and p44 present in the rod, effective deactivation of rhodopsin may occur as a sum of arrestin and p44-mediated deactivation.

ACKNOWLEDGEMENTS

We thank Shenk Co. and Preston Van Hooser for providing bovine retinas for transducin purification preparations. We also thank Yun Ling for helpful discussions and preparation of the manuscript. This research was supported by grants from the National Eye Institute (EY06225, EY08571) and by an unrestricted grant to the Department of Ophthalmology (UF) from Research to Prevent Blindness (to WCS). This work was also supported by NSF-IBN-0119102 (to PRR). The ADVANCE program at University of Maryland Baltimore County (UMBC; grant SBE-0244880) also provided funding for this project from the National Science Foundation (to PRR).

REFERENCES

1. Ridge KD, Abdulaev NG, Sousa M, Palczewski K. Phototransduction: crystal clear. Trends Biochem Sci 2003; 28:479-87. Erratum in: Trends Biochem Sci 2003; 28:526.
2. Makino CL, Wen XH, Lem J. Piecing together the timetable for visual transduction with transgenic animals. Curr Opin Neurobiol 2003; 13:404-12.
3. Arshavsky VY, Lamb TD, Pugh EN Jr. G proteins and phototransduction. Annu Rev Physiol 2002; 64:153-87.
4. Hargrave PA, McDowell JH. Rhodopsin and phototransduction: a model system for G protein-linked receptors. FASEB J 1992; 6:2323-31.
5. Pepe IM. Rhodopsin and phototransduction. J Photochem Photobiol B 1999; 48:1-10.
6. Kuhn H, Cook JH, Dreyer WJ. Phosphorylation of rhodopsin in

bovine photoreceptor membranes. A dark reaction after illumination. Biochemistry 1973; 12:2495-502.
7. McDowell JH, Kuhn H. Light-induced phosphorylation of rhodopsin in cattle photoreceptor membranes: substrate activation and inactivation. Biochemistry 1977; 16:4054-60.
8. Pfister C, Dorey C, Vadot E, Mirshahi M, Deterre P, Chabre M, Faure JP. [Identification of the so-called 48 K protein that interacts with illuminated rhodopsin in retinal rods, and the retinal S antigen, inductor of experimental autoimmune uveoretinitis]. C R Acad Sci III 1984; 299:261-5.
9. Kuhn H, Wilden U. Deactivation of photoactivated rhodopsin by rhodopsin-kinase and arrestin. J Recept Res 1987; 7:283-98.
10. Vishnivetskiy SA, Hirsch JA, Velez MG, Gurevich YV, Gurevich VV. Transition of arrestin into the active receptor-binding state requires an extended interdomain hinge. J Biol Chem 2002; 277:43961-7.
11. Vishnivetskiy SA, Hosey MM, Benovic JL, Gurevich VV. Mapping the arrestin-receptor interface. Structural elements responsible for receptor specificity of arrestin proteins. J Biol Chem 2004; 279:1262-8.
12. Shilton BH, McDowell JH, Smith WC, Hargrave PA. The solution structure and activation of visual arrestin studied by small-angle X-ray scattering. Eur J Biochem 2002; 269:3801-9.
13. Ling Y, Ascano M, Robinson P, Gregurick SK. Experimental and computational studies of the desensitization process in the bovine rhodopsin-arrestin complex. Biophys J 2004; 86:2445-54.
14. Smith WC, Dinculescu A, Peterson JJ, McDowell JH. The surface of visual arrestin that binds to rhodopsin. Mol Vis 2004; 10:392-8.
15. Mendez A, Burns ME, Roca A, Lem J, Wu LW, Simon MI, Baylor DA, Chen J. Rapid and reproducible deactivation of rhodopsin requires multiple phosphorylation sites. Neuron 2000; 28:153-64.
16. Zhang L, Sports CD, Osawa S, Weiss ER. Rhodopsin phosphorylation sites and their role in arrestin binding. J Biol Chem 1997; 272:14762-8.
17. Liu P, Roush ED, Bruno J, Osawa S, Weiss ER. Direct binding of visual arrestin to a rhodopsin carboxyl terminal synthetic phosphopeptide. Mol Vis 2004; 10:712-9.
18. Brannock MT, Weng K, Robinson PR. Rhodopsin's carboxyl-terminal threonines are required for wild-type arrestin-mediated quench of transducin activation in vitro. Biochemistry 1999; 38:3770-7.
19. Hirsch JA, Schubert C, Gurevich VV, Sigler PB. The 2.8 A crystal structure of visual arrestin: a model for arrestin's regulation. Cell 1999; 97:257-69.
20. Avbelj F, Moult J. Determination of the conformation of folding initiation sites in proteins by computer simulation. Proteins 1995; 23:129-41.
21. McDowell JH, Robinson PR, Miller RL, Brannock MT, Arendt A, Smith WC, Hargrave PA. Activation of arrestin: requirement of phosphorylation as the negative charge on residues in synthetic peptides from the carboxyl-terminal region of rhodopsin. Invest Ophthalmol Vis Sci 2001; 42:1439-43.
22. Vishnivetskiy SA, Schubert C, Climaco GC, Gurevich YV, Velez MG, Gurevich VV. An additional phosphate-binding element in arrestin molecule. Implications for the mechanism of arrestin activation. J Biol Chem 2000; 275:41049-57.
23. Smith AM, Klugman KP. "Megaprimer" method of PCR-based mutagenesis: the concentration of megaprimer is a critical factor. Biotechniques 1997; 22:438,442.
24. McDowell JH, Smith WC, Miller RL, Popp MP, Arendt A, Abdulaeva G, Hargrave PA. Sulfhydryl reactivity demonstrates different conformational states for arrestin, arrestin activated by a synthetic phosphopeptide, and constitutively active arrestin. Biochemistry 1999; 38:6119-25.
25. Wessling-Resnick M, Johnson GL. Allosteric behavior in transducin activation mediated by rhodopsin. Initial rate analysis of guanine nucleotide exchange. J Biol Chem 1987; 262:3697-705.
26. Arendt A, McDowell JH, Abdulaeva G, Hargrave PA. Synthesis of multiphosphorylated peptide from a C-terminal bovine rhodopsin sequence. Protein and Peptide Letters 1996; 3:361-8.
27. Laemmli UK. Cleavage of structural proteins during the assembly of the head of bacteriophage T4. Nature 1970; 227:680-5.
28. McDowell JH. Preparing rod outer segment membranes, regenerating and determining rhodopsin concentration. In: Hargrave,P.A., editor. Methods in Neuroscience. San Diego: Academic Press; 1993. p. 123-30.
29. Hanson SM, Francis DJ, Vishnivetskiy SA, Kolobova EA, Hubbell WL, Klug CS, Gurevich VV. Differential interaction of spin-labeled arrestin with inactive and active phosphorhodopsin. Proc Natl Acad Sci U S A 2006; 103:4900-5.
30. Gray-Keller MP, Detwiler PB, Benovic JL, Gurevich VV. Arrestin with a single amino acid substitution quenches light-activated rhodopsin in a phosphorylation-independent fashion. Biochemistry 1997; 36:7058-63.
31. Vishnivetskiy SA, Paz CL, Schubert C, Hirsch JA, Sigler PB, Gurevich VV. How does arrestin respond to the phosphorylated state of rhodopsin? J Biol Chem 1999; 274:11451-4.
32. McDowell JH, Nawrocki JP, Hargrave PA. Phosphorylation sites in bovine rhodopsin. Biochemistry 1993; 32:4968-74.
33. Wilden U, Kuhn H. Light-dependent phosphorylation of rhodopsin: number of phosphorylation sites. Biochemistry 1982; 21:3014-22.
34. Ohguro H, Palczewski K, Ericsson LH, Walsh KA, Johnson RS. Sequential phosphorylation of rhodopsin at multiple sites. Biochemistry 1993; 32:5718-24.
35. Kennedy MJ, Lee KA, Niemi GA, Craven KB, Garwin GG, Saari JC, Hurley JB. Multiple phosphorylation of rhodopsin and the in vivo chemistry underlying rod photoreceptor dark adaptation. Neuron 2001; 31:87-101.
36. Doan T, Mendez A, Detwiler PB, Chen J, Rieke F. Multiple phosphorylation sites confer reproducibility of the rod's single-photon responses. Science 2006; 313:530-3.
37. Pulvermuller A, Maretzki D, Rudnicka-Nawrot M, Smith WC, Palczewski K, Hofmann KP. Functional differences in the interaction of arrestin and its splice variant, p44, with rhodopsin. Biochemistry 1997; 36:9253-60.
38. Granzin J, Wilden U, Choe HW, Labahn J, Krafft B, Buldt G. X-ray crystal structure of arrestin from bovine rod outer segments. Nature 1998; 391:918-21.
39. Dinculescu A, McDowell JH, Amici SA, Dugger DR, Richards N, Hargrave PA, Smith WC. Insertional mutagenesis and immunochemical analysis of visual arrestin interaction with rhodopsin. J Biol Chem 2002; 277:11703-8.
40. Han M, Gurevich VV, Vishnivetskiy SA, Sigler PB, Schubert C. Crystal structure of beta-arrestin at 1.9 A: possible mechanism of receptor binding and membrane Translocation. Structure 2001; 9:869-80.
41. Sommer ME, Smith WC, Farrens DL. Dynamics of arrestin-rhodopsin interactions: arrestin and retinal release are directly linked events. J Biol Chem 2005; 280:6861-71.
42. Ascano M, Robinson PR. Differential phosphorylation of the rhodopsin cytoplasmic tail mediates the binding of arrestin and its splice variant, p44. Biochemistry 2006; 45:2398-407.

43. Humphrey W, Dalke A, Schulten K. VMD: visual molecular dynamics. J Mol Graph 1996; 14:33-8,27-8.

44. Gurevich VV, Chen CY, Kim CM, Benovic JL. Visual arrestin binding to rhodopsin. Intramolecular interaction between the basic N terminus and acidic C terminus of arrestin may regulate binding selectivity. J Biol Chem 1994; 269:8721-7.

The print version of this article was created on 5 Dec 2006. This reflects all typographical corrections and errata to the article through that date. Details of any changes may be found in the online version of the article.